

Investigation into the Chemical Characteristics of Soils near Sinkholes Situated in Anambra State, Nigeria

Chibuogwu IU^{1*}, Ugwu GZ²

¹Nnamdi Azikiwe University Awka, Anambra, Nigeria

²Enugu State University of Science and Technology Agbani, Enugu, Nigeria

DOI: [10.36348/sjce.2023.v07i09.001](https://doi.org/10.36348/sjce.2023.v07i09.001)

| Received: 24.08.2023 | Accepted: 29.09.2023 | Published: 09.10.2023

*Corresponding author: Chibuogwu IU

Nnamdi Azikiwe University Awka, Anambra, Nigeria

Abstract

In this comprehensive study, we delve into the chemical properties of soil in the proximity of sinkholes located in Anambra state of Nigeria. Three distinct sinkhole sites were selected for examination: Awka site 1 (6.2232°N and 7.0824°E), Awka site 2 (6.2220°N and 7.0819°E), and Agulu (6.0941°N and 7.0203°E). For a comprehensive analysis, 24 soil samples were meticulously collected and subjected to thorough analysis. These samples comprised of 15 specimens obtained from the immediate vicinity of the sinkholes, while 9 samples were procured from locations situated at least 2 kilometers away from the sinkhole sites. The study focused on investigating various parameters, namely pH levels, Organic Carbon (OC) content, Organic Matter (OM) content, Aluminum (Al) levels, Hydrogen (H) levels, Total Nitrogen (TN) content, Magnesium (Mg) levels, Potassium (K) levels, Sodium (Na) levels, Calcium (Ca) levels, Effective Cation Exchange Capacity (ECEC), Base Saturation, and soil texture. The obtained results revealed that the study areas predominantly exhibited a sandy composition with a notably low clay content. Furthermore, the analysis indicated low hydrogen values, while sodium levels were observed to be relatively high. Consequently, certain areas, particularly those situated farther away from the sinkhole site, exhibited a reduced amount of exchangeable bases and effective cation exchange capacity. This phenomenon potentially resulted in leaching and dispersion within the soil, leading to inadequate water infiltration and subsequent run-off. Notably, this process may have contributed to the formation of tunnel erosion, ultimately resulting in the emergence of sinkholes.

Keywords: Tunnel erosion, Sinkhole, Dispersion, Leaching and Sodidity.

Copyright © 2023 The Author(s): This is an open-access article distributed under the terms of the Creative Commons Attribution 4.0 International License (CC BY-NC 4.0) which permits unrestricted use, distribution, and reproduction in any medium for non-commercial use provided the original author and source are credited.

INTRODUCTION

Soil, a vital and finite resource present on the Earth's surface, plays a pivotal role in sustaining human existence and facilitating plant growth. Erosion, a natural process, poses a significant threat to the integrity of soils [1, 2]. It is through the forces of running water and wind that soils become dislodged and transported, giving rise to various forms of erosion, namely gully, sheet, and tunnel erosions. While gully and sheet erosions manifest on the surface, their formation processes are discernible to the naked eye [3]. In contrast, tunnel erosion occurs clandestinely beneath the Earth's surface, concealed from immediate observation [4]. Tunnel erosion is primarily initiated by the infiltration of water, which diligently navigates its way through the labyrinthine network of soil pores [5]. This water, while on its subterranean journey, carries with it minute particles, thereby initiating the formation of tunnel erosion [6]. It commences as a diminutive orifice, often referred to as a

flute hole [6], delicately etched upon the terrestrial canvas. With the passage of time, this incipient hole gradually expands, evolving into an indeterminate diameter, eventually assuming the form of a pipe-like structure [3, 7]. The erosive consequences stemming from the development of tunnels can result in the formation of cavities, which, if left unattended, may precipitate the occurrence of a sinkhole—an insidious manifestation of subsurface erosion. Due to the covert nature of tunnel erosion's progression and its potential for causing significant damage, it is widely regarded as the most treacherous form of erosion, necessitating diligent efforts to trace and control its pernicious effects [8]. The dispersion of soil arising from the phenomenon of soil sodicity emerges as the primary factor contributing to the inherent vulnerability of soils towards tunnel erosion [9]. Sodic soils, prevalent in regions characterized by elevated levels of sodium and other exchangeable cations, exhibit a general predisposition towards this

form of soil degradation[10]. The process of soil dispersion instigates the entrapment of clay particles within soil pores, leading to a compaction of the soil matrix and impeding water infiltration [11]. Consequently, the ensuing runoff, laden with fine particles and other substances, exacerbates the erosive potential of the environment [9-11]. The rate of tunnel erosion is intricately influenced by the rate of water infiltration, a crucial factor warranting careful consideration. Water infiltration refers to the maximum rate at which a soil, under specific conditions and at a given moment, can absorb excess water applied to its surface, be it in the form of rainfall or shallow impounded water. It is important to note that the infiltration rate of a soil is not typically characterized by a discrete value, but rather by a graph illustrating the relationship between the rate of water entry and the elapsed time since infiltration commenced[12]. This graph typically exhibits a rapid decrease in the rate of entry over time. Therefore, the term "infiltration rate" encompasses both the magnitude of intake rate values and the shape of the infiltration rate versus time curve, encapsulating the dynamic nature of this phenomenon [12].

While some researchers have sought to characterize a given soil or soil surface condition by employing a "final" or "equilibrium" infiltration rate, which represents a constant value attained over time [12-14], such an approach provides only limited information and proves inadequate for most practical applications. A poor rate of infiltration can have perilous consequences, as it engenders the potential for flooding and runoff. The movement of runoff water follows a diffusion pattern,

migrating from regions characterized by low infiltration rates towards areas with higher infiltration rates. As this water traverses, it carries with it debris and fine particles, gradually forming tunnels within the subsurface by exploiting regions of higher infiltration rates. Anambra State, an enchanting state nestled in the southeastern region of Nigeria, has been grappling with a series of sinkhole incidents in recent years [15]. These unsettling occurrences have not only inflicted substantial infrastructural damages but also posed a significant risk to the local communities. Hence, it becomes imperative for us, as scholars and researchers, to embark upon a rigorous chemical investigation of the soils surrounding these sinkholes. By delving deep into the intricacies of their causative factors, we can gain a profound understanding of their genesis and, in turn, evaluate the potential risks they impose. The dynamic nature of sinkholes demands a comprehensive and multidisciplinary approach. From geological and hydrogeological analyses to chemical assessments, a meticulous investigation will provide us with invaluable insights into the underlying mechanisms that trigger these phenomena. By unraveling the intricate interplay between the geological formations, hydrological processes, and chemical composition of the soils, we can commence the journey towards formulating effective mitigation strategies and ensuring the safety and well-being of the affected communities. This research is elated to analyse the chemical role of soil to the prevalence occurrence of sinkholes in Anambra state, Nigeria.

Study Area

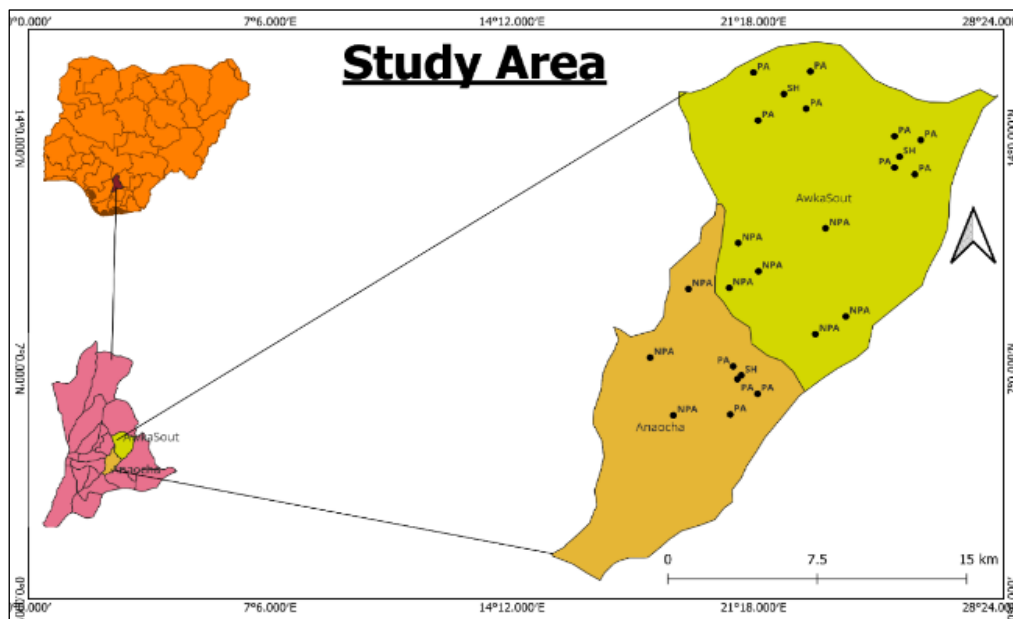


Figure 1: The study area with an insert of Anambra state and Nigeria (PA = Piping Area, NPA = Non-piping area)

In this study, our focus is on two specific sites within the Awka South area and one site in the Aniocha Local Government area of Anambra State, Nigeria (as shown in Figure 1). The first site, Awka Site 1, is situated at coordinates (6.2232°N and 7.0824°E). Here, a soil pipe with a diameter of approximately 5cm has caused significant damage to a constructed road. This damage has resulted in the formation of double sinkholes, each with a diameter of around 70cm (refer to Figure 2a). The Awka Site 2, located at coordinates (6.222°N and 7.0819°E), we find a soil pipe that has been present for

approximately three years. This pipe has caused the formation of multiple holes, each with an average diameter of 10cm, as well as a visible sinkhole measuring around 100cm in diameter (as depicted in Figure 2b). Lastly, our third site is situated in Agulu, with geographical coordinates (6.0941°N and 7.0203°E). By closely examining these three sites, we aim to gain a deeper understanding of the characteristics and formation mechanisms of soil pipes in areas prone to sinkholes.



Figure 2: (a) Sinkhole at Awka site 1 (b) Soil pipe at Awka site 2

Geology of Anambra state

Anambra State, located in the southern part of Nigeria, occupies a geographical area of latitude 5.7503°N and 6.7503°N, and longitude 7.2502°E and 7.7502°E. It is an integral part of the Anambra Sedimentary Basin, which is situated in the southern region of Nigeria (as illustrated in figure 3). The state covers an expansive area of approximately 40,000 square kilometers, as documented by [15] and [4]. The southern boundary of the Anambra Basin aligns with the delta swamps of the Niger Delta Basin, extending northwards beyond the Bende Ameki Formation [16, 17]. It is widely believed that the formation of the basin occurred concurrently with the folding and uplift of the Abakaliki-Benue area during the Santonian era [18]. Consequently, the Anambra Basin serves as a significant center for the deposition of clastic deposits and deltaic sequences [18]. These formations are a result of tectonic activity within the second Lower Benue Trough, which played a crucial role in the geological evolution of the area (see figure 3) [16]. Anambra basin boasts of a geological composition that is rich in ancient Cretaceous delta deposits, constituting the sedimentary rocks found within the

region. The basin is predominantly characterized by the Nnaka Sand, which dates back to the Eocene period [16, 18]. Overlying this sandy formation is the paralic Ogwashi-Asaba formation, originating from the Oligocene epoch. On the other hand, the marine Imo shale underlies a significant portion of the basin [18]. It is worth noting that the presence of these sands, primarily the coastal plain sands, has contributed to ecological challenges in the area. These sands exhibit a high susceptibility to erosion, leading to severe ecological problems within the region. Underneath the weak lateritic and acidic soils lie unstable and poorly consolidated geological rocks and materials [17, 18]. The sandy components of these geological units house substantial groundwater reservoirs, known as aquifers [4]. However, these aquifers pose a threat when subjected to excessive pore water pressures, especially when overlying structures bear uncompromising loads [15]. In addition to these geological characteristics, the lateritic and sandy soils are highly vulnerable to erosion caused by storm water runoff. This erosion can further exacerbate the ecological issues faced by the region.

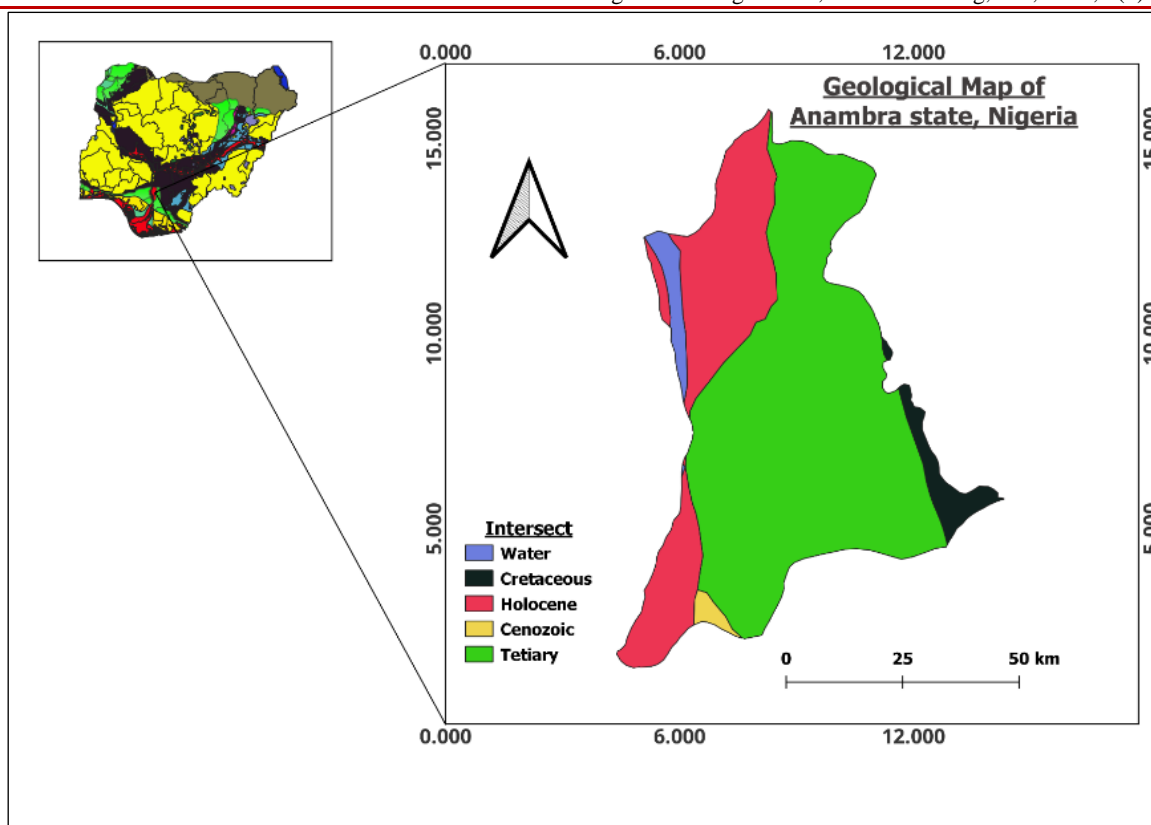


Figure 3: Geology of Anambra State, Nigeria

MATERIALS & METHODS

To conduct this research, the following materials were utilized: auger, spade, container for soil samples, refrigerator (for sample storage), oven (for drying sampled soils), pestle, a 2mm and 0.5mm mesh sieves for soil sieving, weighing balance. The parameters examined in this study include pH, Organic Carbon (OC), Organic Matter (OM), Aluminum (Al), Hydrogen (H), Total Nitrogen (TN), Magnesium (Mg), Potassium (k), Sodium (Na), Calcium (ca), Effective Cation Exchange Capacity, Base Saturation and soil texture. In order to determine the values of the various parameters mentioned above, 24 soil samples were collected from both sinkhole-affected localities and unaffected sections of the study area. The samples were taken at a depth of 0-5ft. Specifically, 15 samples were collected from the piping area (PA) with sinkholes (SH), and 9 samples were collected approximately 20km away from a known piping area (non-piping area, NPA). The locations where each samples were gotten are labeled using alphabetic notations A1 – A5 are site within the sinkhole vicinity in Awka site 1, A6 – A8 are sit far from the sinkhole, B1 – B5 are site at Awka site 2, within the sinkhole vicinity while B6 – B8 are distance site from the sinkhole. The alphabet C is used to denote the same approach for the Agulu site.

Analysis of Soil Samples

The following steps were taken to analyze the soil samples:

1. Soil samples were spread in a petri dish and dried in an oven at 105°C for a duration of 4 hours.
2. The dried soil samples were then ground and passed through a 2mm mesh aluminum sieve. Soil samples smaller than 2mm were stored in polythene bags for subsequent analysis.
3. The pH values of the soil samples were determined using the procedure outlined by [19]. 20g of soil was added to a 50mL beaker, followed by the addition of 20mL of distilled water. The suspension was stirred for 5 minutes and then allowed to settle for 1 hour to enable the clay particles to settle. The pH readings were obtained using a Mettler Toledo Seven Easy pH Meter.

The values of soil organic carbon and organic matter were determined using the Walkley-Black method [19]. The prepared dried samples were further sieved, and 1g of the 0.5mm sample fraction was weighed and transferred into a conical flask. A measured amount of potassium dichromate ($K_2Cr_2O_7$) and sulfuric acid (H_2SO_4) were added to the sample, resulting in an exothermic reaction. The solutions, one with the soil sample and one without, were allowed to cool in a ventilated environment. Subsequently, 100mL of

distilled water was added to each solution, generating heat. The cooled samples were titrated using three drops of ferroin as an indicator against Ferrous Sulphate solution until a maroon color end-point was observed. A blank titration was conducted at the beginning without the soil solution. The equation below is then used to obtain the percentage of organic carbon.

$$\%Organic\ Carbon = \frac{10(B - T)}{B \times 0.03 \times 100s}$$

B = titre value of blank sample in mL.

T = titre sample for soil sample in mL.

S = weight of soil in gram

$$\%Organic\ Matter = \%Organic\ Carbon \times 1.729$$

4. For the value of soil moisture content, the weight of the wet the soil content and container were gotten using the gravimetric method. The weight in which the sample was to be placed and the sample were oven dried for 24 hours separately. The weight of the container and the weight of the container when the sample was placed in it were measured respectively. The water content of the soil (ω) is obtained using the relation below.

$$\% \omega = \frac{W_2 - W_3}{W_3 - W_1}$$

W_1 = Weight of container

W_2 = weight of container + weight of moist soil

W_3 = weight of container + weight of dry soil

5. For the particle size analysis, the Bouyoucous Hydrometer method of [19] was used to determine particle size distribution. The dried sieved 2mm soil samples were weighed and transfer into a beaker. Each soil sample received a calgon solution (sodium hexametaphosphate) that was left to spread and penetrate the samples for 24 hours. The dispersed calgon oiled samples were moved into a 1000mL measuring cylinder and filled with 950mL of distilled water. The soil hydrometer and thermometer were used to take the first reading after each 40 seconds to obtain H_1 and T_1 . The measuring cylinder containing the soil mixture was allowed to stand for 2 hours to determine H_2 and T_2 . The particle size distribution was then calculated using equations below

$$\%sand = 100 - (H_1 + 0.2(T_1 - 68) - 2)2$$

$$\%clay = (H_2 + 0.2(T_2 - 68) - 2)2$$

$$\%slit = 100 - (\%clay + \%sand)$$

6. Analytical Techniques for Chemical Parameter Determination. To ascertain the levels of calcium and magnesium in the exchange bases, we utilized the esteemed complex metric titration method, as outlined by Jackson in 1958. The titrimetric method, as established

by Mclean in 1982, is used to ascertain the levels of exchange hydrogen and aluminum. This meticulous approach affords us the opportunity to discern their intricate nuances of these components, unraveling their significance in the broader chemical context. To determine the levels of sodium and potassium, we harnessed the power of the flame photometer. This innovative instrument allows for accurate measurement of these elements. The effective exchange capacity, a critical parameter in our investigation, was determined by summing the values of all exchange bases, including calcium, magnesium, sodium, and potassium. We employed the micro-Kjeldahl digestion method, as outlined by Bremner and Mulvaney in 1982, to determine the value of nitrogen. Finally, to calculate the base saturation, a vital metric in our analysis, we adopted the methodology proposed by [20].

RESULTS

To study the intricate nature of the soil composition within the study area, we embarked upon a meticulous analysis of various soil textures at different depths, starting from the surface. The culmination of this analysis is presented in Table 1, Figure 4a, and Figure 4b, which provide a visual representation of our findings. The mean value of sand content ranges between 69.7% and 81.2%. In addition to the abundance of sandy soil, our analysis also reveals the presence of an low amount of clay soils. This secondary component, with a mean value ranging from 14.8% to 24.2%, contributes to the overall soil composition. Furthermore, there is a notably very low amount of silt soils, ranging from 1.3% to 6.4%. This relatively modest presence of clay further accentuates the sandy nature of the study area, while simultaneously raising intriguing questions about the underlying geological processes and their influence on soil formation. From the soil textural analysis, figure 9b shows that the soil in the study area falls within sandy loam for area located particularly on the non-piping sides of the research area. The loam sandy, sandy loam and sandy clay loam characterized the textural class of the piping region (see figure 9a). The results presented in Table 2, Figure 5a, and Figure 5b show the mean values of organic carbon, organic matter, and total nitrogen at varying depths from the surface within the study area. The content of organic carbon spans a range from 0.15% to 0.83%. Notably, the highest concentration of organic carbon is observed at location C6, which intriguingly belongs to a non-piping region and the lowest concentration of organic carbon is found at location A2, situated within a piping region. Similarly, our evaluation of organic matter reveals a mean value range spanning from 0.26% to 0.83% at different depths. Remarkably, the highest and lowest values of organic matter align with those obtained for organic carbon. This correlation arises from the direct derivation of organic matter values from organic carbon measurements. The analysis of total

nitrogen values within the areas show values ranging from 0.05 cmol/kg to 0.67 cmol/kg. Notably, the lowest value of total nitrogen is located at C2, a piping region at the Agulu site. Conversely, the highest value of total nitrogen is recorded at B7, a non-piping region at Awka site 2.

A comprehensive analysis of soil characteristics within the study area has yielded valuable insights, as presented in Table 3, Figure 6a, and Figure 6b. These findings provide a comprehensive overview of the mean values of soil pH, aluminum, and hydrogen at various depths. The evaluation of soil pH has revealed a range spanning from 4.3 cmol/kg to 7.2 cmol/kg, indicating a spectrum that encompasses both acidic and alkaline conditions. This wide range of pH values underscores the diverse nature of the study area's soil composition. Notably, the lowest pH value is observed at location A1, which intriguingly corresponds to a sinkhole. Contrarily, the highest pH value is recorded at location A8, situated within a non-piping region. Our investigation of aluminum levels in the soil has yielded mean values ranging from 0.43 cmol/kg to 1.76 cmol/kg. Remarkably, the highest and lowest aluminum values are encountered at Awka site 1, with the lowest value detected within the sinkhole at A1, and the highest value observed in a non-piping region. Additionally, the average hydrogen levels range from 0.26 cmol/kg to 1 cmol/kg, revealing notable variations across the study area. The highest hydrogen value is observed within the sinkhole at Awka site 2, while the lowest value is found in the piping region A4 of Awka site 1. Furthermore, unique hydrogen values are also identified in regions B2 and A1, both situated within Awka site 2 and exhibiting a hydrogen value of 0.9 cmol/kg. A comprehensive examination into the levels of potassium, sodium, and calcium at varying depths, is illustrated in Table 4, Figure 7a, and Figure 7b. The assessment of potassium levels reveals a range spanning from 0.13 cmol/kg to 0.69 cmol/kg. The lowest potassium value is observed in the non-piping region of A8 at Awka site 1, while the highest value is found in C6 at the Agulu site. For sodium content, we find that the values range from 0.15 cmol/kg to 2.36 cmol/kg across the three investigated sites. The highest sodium values are observed in C5, a non-piping region at the Agulu site, while the lowest value of 0.15 cmol/kg is found in the sinkhole investigated at Awka site 2. The average calcium value ranges from 0.2 cmol/kg to 2.07 cmol/kg, with notable disparities observed across different locations. The sinkhole of C1 at the Agulu site exhibits the lowest calcium value, while the piping area of C5 within the same Agulu site boasts the highest calcium value.

Table 5, Figure 8a, and Figure 8b provide a comprehensive depiction of the values obtained for magnesium, effective cation exchange capacity (ECEC), and base saturation at various depths from the surface within the study areas. Examining the levels of magnesium, we observe an average value ranging from 0.3 cmol/kg to 1.9 cmol/kg across different depths. The piping area of A2 in Awka site 2 exhibits the lowest magnesium value, while the highest value is found at C4 in the Agulu site. For the analysis of effective cation exchange capacity (ECEC), which parameter is derived from the sum of all exchange bases present in the study areas. The mean ECEC values at different depths range from 1.58 cmol/kg to 6.27 cmol/kg. The lowest and highest ECEC values are observed at A2 and A8, both located in Awka site 1. Furthermore, the analysis of base saturation reveals mean values ranging from 17.2 % to 56.6 % across different depths within the study areas. Notably, the highest base saturation value is located at A6 in Awka site 1, while the lowest value is found at C4 in the Agulu site. It is worth noting that the Agulu site exhibits the highest concentrations of total sodium and base salt.

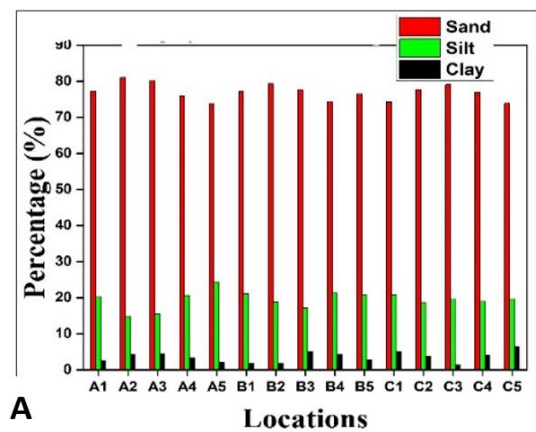


Figure 4: (a) A graph soil texture at the piping area

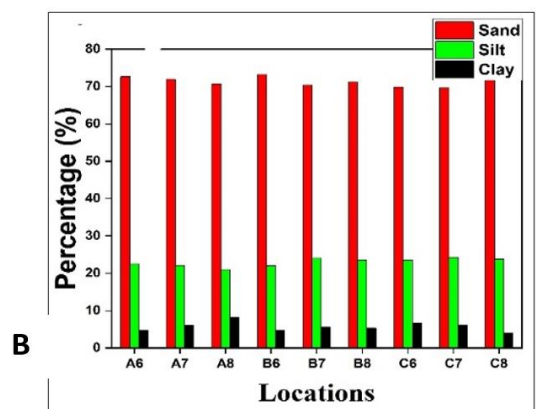


Figure 4: (b) A graph of soil texture at the non-piping area

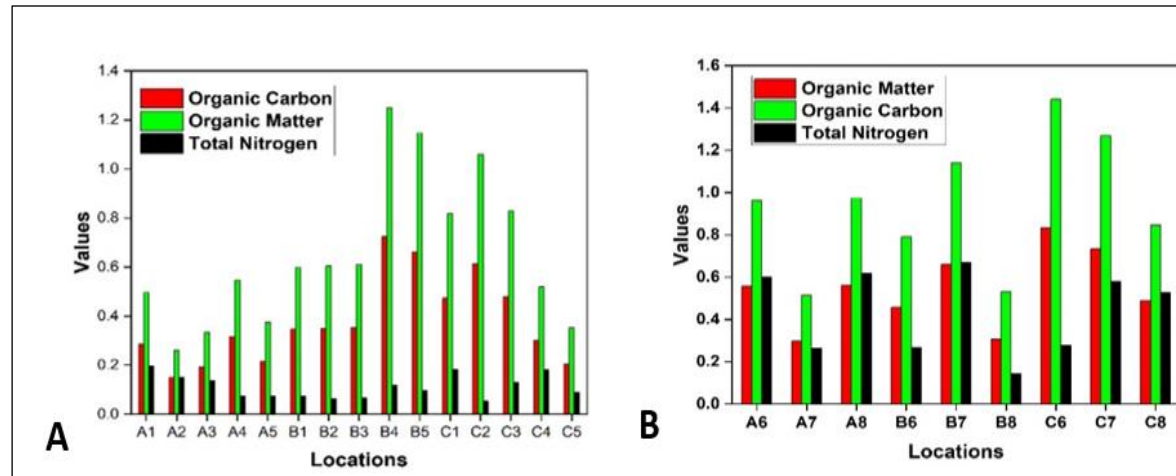


Figure 5: (a) A graph of OC, OM and TN at the piping area (b) A graph of OC, OM and TN at the non-piping area

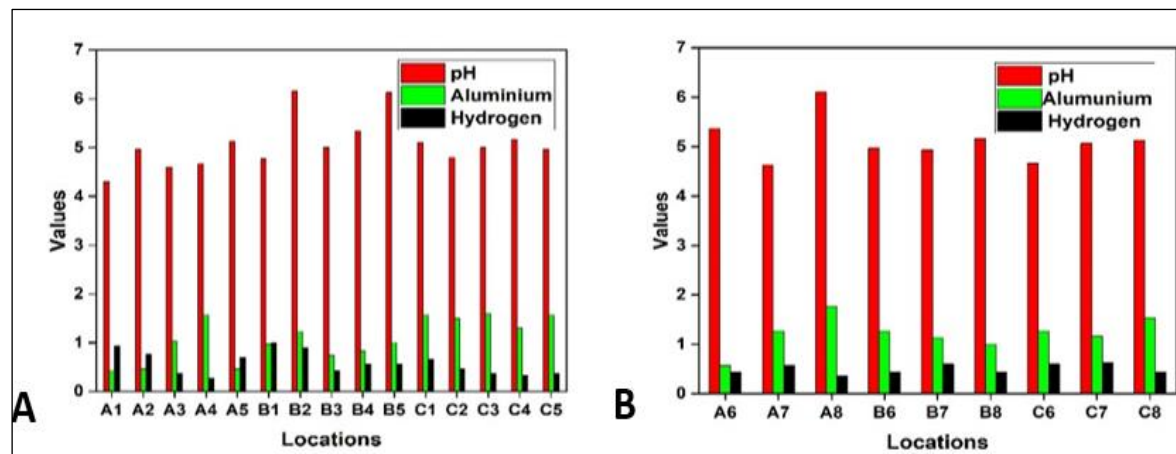


Figure 6: (a) A graph of pH, Al and H at the piping area (b) A graph of pH, Al and H at the non-piping area

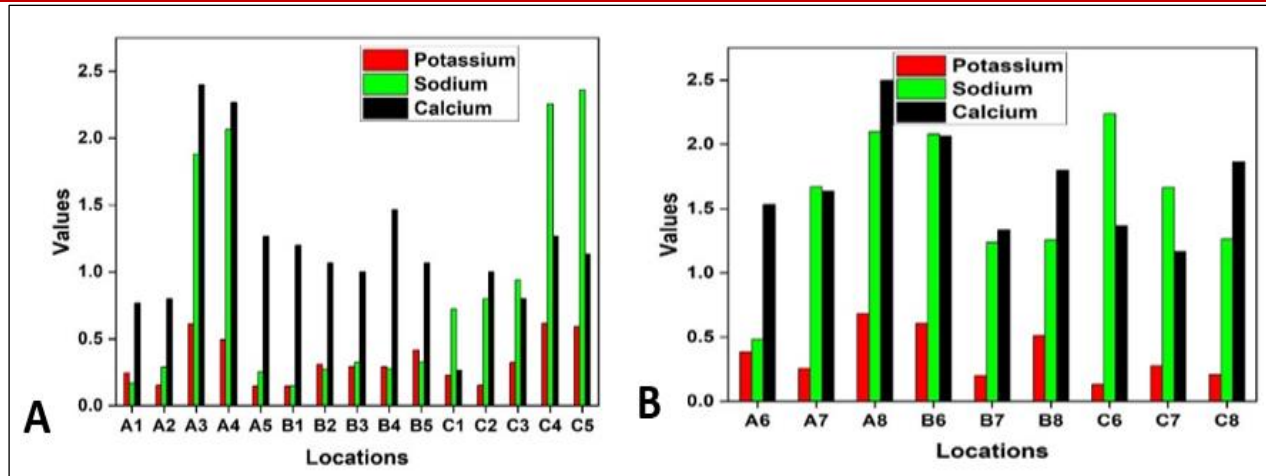


Figure 7: (a) A graph of K, Na and Ca at the piping area (b) A graph of K, Na and Ca at the non-piping area

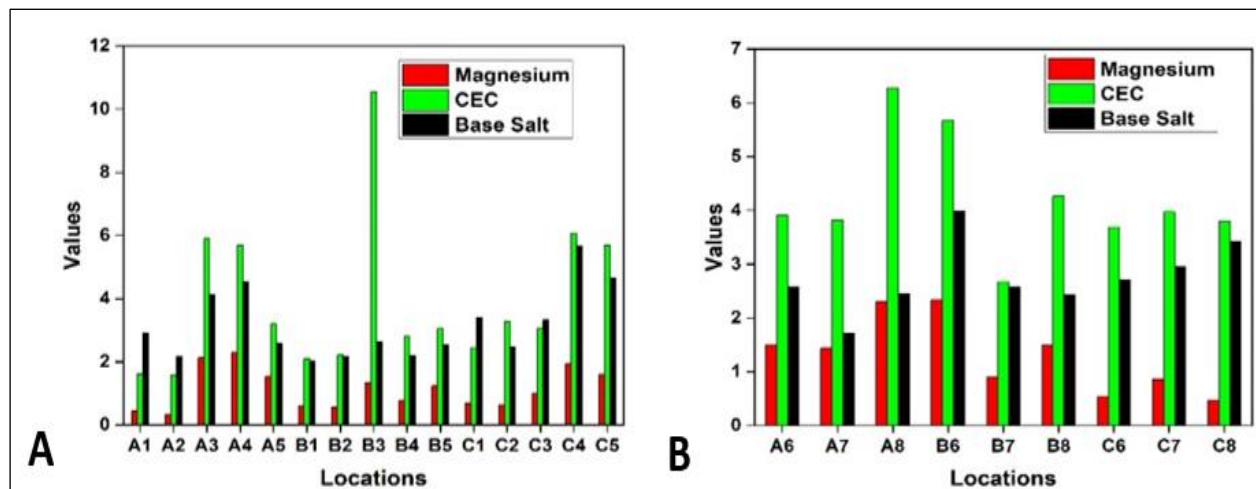


Figure 8: (a) A graph of Mg, ECEC and Base Sat at the piping area (b) A graph of Mg, Mg and Base Sat at the non-piping area

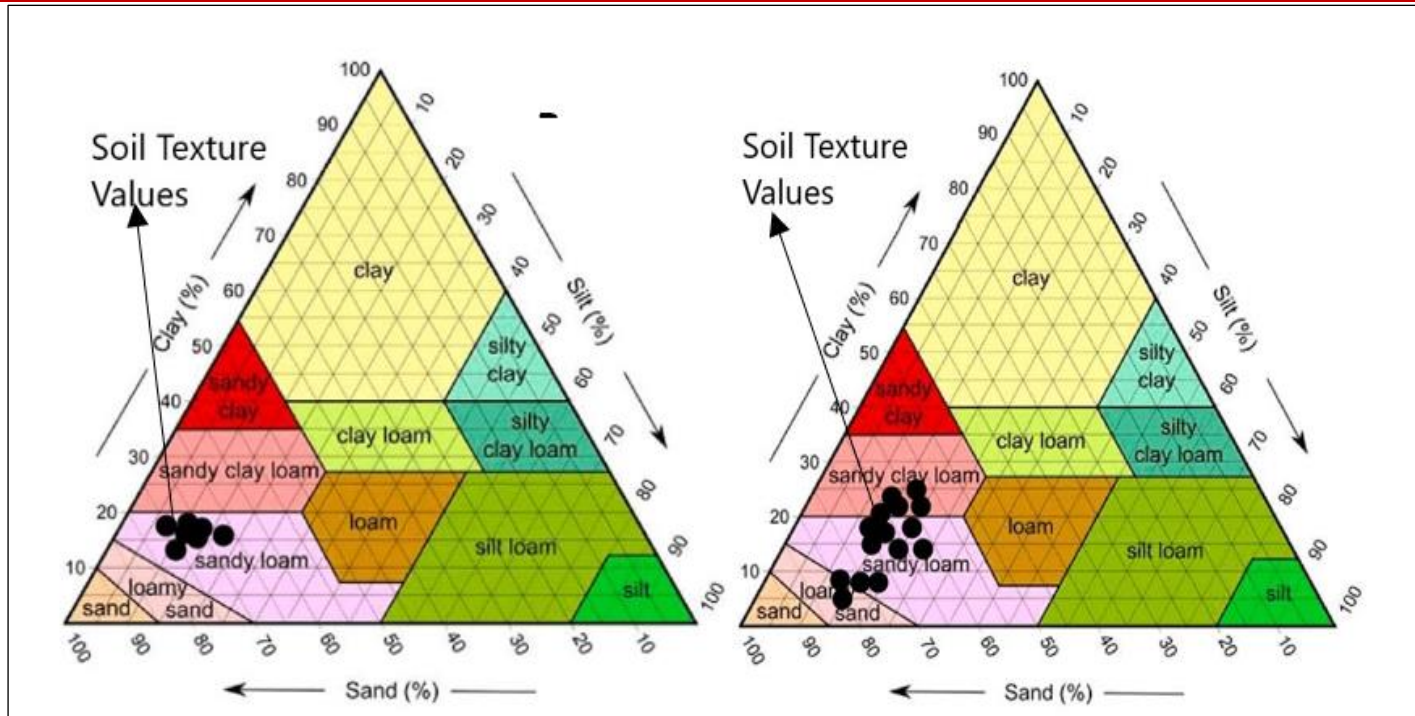


Figure 9: Ternary graph for soil particle at the piping region (b) Ternary graph for soil particle at the piping region

Table 1: Mean Values of soil texture at different Soil Depth

S/N	Code	Elevation	Latitude	Longitude	Sand (%)			Mean	Clay (%)			Mean	Silt (%)			Mean	Remark
					Soil Depth (ft.)				Soil Depth (ft.)				Soil Depth (ft.)				
					0.5	1.5	2.5		0.5	1.5	2.5		0.5	1.5	2.5		
1	A1	212.9	6.1967	7.0959	85.2	72.3	74.2	77.2	14	23.6	23.1	20.2	0.8	4.1	2.7	2.5	SH
2	A2	216.3	6.1916	7.0936	80.4	83	79.5	81.0	15.9	14.1	14.4	14.8	3.7	2.9	6.1	4.2	PA
3	A3	218.2	6.1884	7.1028	81.3	78.1	81.2	80.2	18.5	17.5	10.2	15.4	0.2	4.4	8.6	4.4	PA
4	A4	209.8	6.2063	7.0936	79	74	75	76.0	19.2	22.3	20.4	20.6	1.8	3.7	4.6	3.4	PA
5	A5	210.1	6.2045	7.1055	72	70.3	79	73.8	25.2	27.4	20.1	24.2	2.8	2.3	0.9	2.0	PA
6	A6	229.9	6.1134	7.0577	70	75	73	72.7	23.2	22.1	22.4	22.6	6.8	2.9	4.6	4.8	NPA
7	A7	225.8	6.1217	7.0715	73.2	67.2	75.3	71.9	23.2	26.6	16.5	22.1	3.6	6.2	8.2	6.0	NPA

S/N	Code	Elevation	Latitude	Longitude	Sand (%)			Mean	Clay (%)			Mean	Silt (%)			Mean	Remark
					Soil Depth (ft.)				Soil Depth (ft.)				Soil Depth (ft.)				
					0.5	1.5	2.5		0.5	1.5	2.5		0.5	1.5	2.5		
8	A8	216.8	6.1631	7.0623	69	70.1	73	70.7	22.5	20.1	20.4	21.0	8.5	9.8	6.6	8.3	NPA
9	B1	199	6.2261	7.0434	74	78	79.3	77.1	24.2	20.6	18.5	21.1	1.8	1.4	2.2	1.8	SH
10	B2	200.3	6.2367	7.0554	83.2	77.5	77.1	79.3	16.1	21.1	19.3	18.8	0.7	1.4	3.6	1.9	PA
11	B3	199.4	6.2362	7.0296	75	80.1	78.2	77.8	22.2	14.1	15.3	17.2	2.8	5.8	6.5	5.0	PA
12	B4	204.3	6.2192	7.0535	75.4	78.2	69.4	74.3	20.1	16.8	27.3	21.4	4.5	5	3.3	4.3	PA
13	B5	206.2	6.2137	7.0317	77.2	79	73.2	76.5	20.8	18.2	23.2	20.7	2	2.8	3.6	2.8	PA
14	B6	229.1	6.1562	7.0227	73	75.1	71.6	73.2	22.5	19.4	24.1	22.0	4.5	5.5	4.3	4.8	NPA
15	B7	227.1	6.1429	7.0319	69.2	75.6	66.3	70.4	24.1	22.1	26.1	24.1	6.7	2.3	7.6	5.5	NPA
16	B8	231.6	6.1351	7.0186	70.1	70.5	73.1	71.2	26.2	24.2	20.1	23.5	3.7	5.3	6.8	5.3	NPA
17	C1	237.1	6.0941	7.0241	70.2	77.4	75.1	74.2	22.1	20.1	20.3	20.8	7.7	2.5	4.6	4.9	SH
18	C2	238.2	6.0923	7.0223	83.2	70.5	79.3	77.7	12.5	24.2	19.2	18.6	4.3	5.3	1.5	3.7	PA
19	C3	230.1	6.0983	7.0204	88.5	74.5	74.1	79.0	11.2	23.7	24.2	19.7	0.3	1.8	1.7	1.3	PA
20	C4	242.1	6.0854	7.0315	79.2	75.4	76.4	77.0	19.5	19.3	18.2	19.0	1.3	5.3	5.4	4.0	PA
21	C5	244.4	6.0757	7.0191	75.2	69.3	77.2	73.9	19.2	27.1	12.9	19.7	5.6	3.6	9.9	6.4	PA
22	C6	240	6.1346	7.0001	70.1	68.3	71.2	69.9	22.1	26.4	22.1	23.5	7.8	5.3	6.7	6.6	NPA
23	C7	241.4	6.1024	6.9827	69	73.7	66.3	69.7	23.3	22.1	27.2	24.2	7.7	4.2	6.5	6.1	NPA
24	C8	241	6.0753	6.9933	70.1	67.5	79.1	72.2	23.1	28.1	20.2	23.8	6.8	4.4	0.7	4.0	NPA

Table 2: Mean Values of Organic Carbon, Organic Matter and Total Nitrogen at different Soil Depth in cmol/kg

S/N	Code	Elevation	Latitude	Longitude	Organic Carbon				Organic Matter				TN				Remark
					Soil Depth(ft)			Mean	Soil Depth (ft)			Mean	Soil Depth (ft)			Mean	
					0.5	1.5	2.5		0.5	1.5	2.5		0.5	1.5	2.5		
1	A1	212.9	6.1967	7.0959	0.51	0.22	0.13	0.286667	0.88	0.38	0.22	0.495647	0.3	0.2	0.09	0.196667	SH
2	A2	216.3	6.1916	7.0936	0.22	0.14	0.09	0.15	0.38	0.24	0.16	0.25935	0.2	0.2	0.05	0.15	PA
3	A3	218.2	6.1884	7.1028	0.31	0.18	0.09	0.193333	0.54	0.31	0.16	0.334273	0.3	0.09	0.02	0.136667	PA
4	A4	209.8	6.2063	7.0936	0.62	0.3	0.03	0.316667	1.07	0.52	0.05	0.547517	0.1	0.07	0.05	0.073333	PA
5	A5	210.1	6.2045	7.1055	0.42	0.18	0.05	0.216667	0.73	0.31	0.09	0.374617	0.12	0.08	0.02	0.073333	PA
6	A6	229.9	6.1134	7.0577	1.34	0.21	0.12	0.556667	2.32	0.36	0.21	0.962477	0.7	0.8	0.3	0.6	NPA
7	A7	225.8	6.1217	7.0715	0.61	0.21	0.07	0.296667	1.05	0.36	0.12	0.512937	0.7	0.07	0.02	0.263333	NPA
8	A8	216.8	6.1631	7.0623	1.02	0.53	0.14	0.563333	1.76	0.92	0.24	0.974003	0.9	0.5	0.45	0.616667	NPA
9	B1	199	6.2261	7.0434	0.61	0.33	0.1	0.346667	1.05	0.57	0.17	0.599387	0.1	0.05	0.07	0.073333	SH
10	B2	200.3	6.2367	7.0554	0.71	0.21	0.13	0.35	1.23	0.36	0.22	0.60515	0.08	0.08	0.03	0.063333	PA
11	B3	199.4	6.2362	7.0296	0.52	0.41	0.13	0.353333	0.90	0.71	0.22	0.610913	0.1	0.05	0.05	0.066667	PA
12	B4	204.3	6.2192	7.0535	1.21	0.81	0.15	0.723333	2.09	1.40	0.26	1.250643	0.84	0.5	0.39	0.576667	PA
13	B5	206.3	6.2137	7.0317	1.02	0.72	0.25	0.663333	1.76	1.24	0.43	1.146903	0.7	0.8	0.02	0.506667	PA

S/N	Code	Elevation	Latitude	Longitude	Organic Carbon				Organic Matter				TN				Remark
					Soil Depth(ft)			Mean	Soil Depth (ft)			Mean	Soil Depth (ft)			Mean	
					0.5	1.5	2.5		0.5	1.5	2.5		0.5	1.5	2.5		
14	B6	229.1	6.1562	7.0227	0.91	0.43	0.03	0.456667	1.57	0.74	0.05	0.789577	0.5	0.2	0.1	0.266667	NPA
15	B7	227.1	6.1429	7.0319	1.08	0.7	0.2	0.66	1.87	1.21	0.35	1.14114	0.8	0.71	0.5	0.67	NPA
16	B8	231.6	6.1351	7.0186	0.51	0.31	0.1	0.306667	0.88	0.54	0.17	0.530227	0.2	0.15	0.08	0.143333	NPA
17	C1	231.1	6.0941	7.0241	1.12	0.21	0.09	0.473333	1.94	0.36	0.16	0.818393	0.2	0.15	0.2	0.183333	SH
18	C2	238.2	6.0923	7.0223	1.21	0.43	0.2	0.613333	2.09	0.74	0.35	1.060453	0.08	0.05	0.03	0.053333	PA
19	C3	230.1	6.0983	7.0204	0.84	0.51	0.09	0.48	1.45	0.88	0.16	0.82992	0.2	0.17	0.02	0.13	PA
20	C4	242.1	6.0854	7.0315	0.63	0.22	0.05	0.3	1.09	0.38	0.09	0.5187	0.3	0.21	0.03	0.18	PA
21	C5	244.4	6.0757	7.0191	0.41	0.15	0.05	0.203333	0.71	0.26	0.09	0.351563	0.14	0.1	0.03	0.09	PA
22	C6	240.1	6.1346	7.0001	1.31	0.89	0.3	0.833333	2.26	1.54	0.52	1.440833	0.42	0.3	0.11	0.276667	NPA
23	C7	241.4	6.1024	6.9827	1.05	0.9	0.25	0.733333	1.82	1.56	0.43	1.267933	0.48	0.57	0.69	0.58	NPA
24	C8	241.5	6.0753	6.9933	0.9	0.52	0.05	0.49	1.56	0.90	0.09	0.84721	0.51	0.47	0.6	0.526667	NPA

Table 3: Mean Values of pH (no unit), Aluminum and Hydrogen at different depth in cmol/kg

S/N	Code	Elevation	Latitude	Longitude	pH			Mean	Al			Mean	H			Mean	Remark
					Soil Depth (ft)				Soil Depth (ft)				Soil Depth (ft)				
					0.5	1.5	2.5	0.5	1.5	2.5	0.5	1.5	2.5				
1	A1	212.9	6.1967	7.0959	4.1	4.8	4	4.3	0.6	0.4	0.3	0.433333	1	0.8	1	0.933333	SH
2	A2	216.3	6.1916	7.0936	4.8	5.4	4.7	4.966667	0.4	0.1	0.9	0.466667	0.8	0.6	0.9	0.766667	PA
3	A3	218.2	6.1884	7.1028	7.1	7	7.1	7.066667	1.3	0.9	0.9	1.033333	0.4	0.2	0.5	0.366667	PA
4	A4	209.8	6.2063	7.0936	6.8	6.7	6.6	6.7	1.9	1.3	1.5	1.566667	0.5	0.2	0.1	0.266667	PA
5	A5	210.1	6.2045	7.1055	5.1	5.6	4.7	5.133333	0.5	0.5	0.4	0.466667	0.7	0.5	0.9	0.7	PA
6	A6	229.9	6.1134	7.0577	5.8	5.1	5.2	5.366667	0.7	0.7	0.3	0.566667	0.6	0.4	0.3	0.433333	NPA
7	A7	225.8	6.1217	7.0715	5.5	6.9	5.7	6.033333	1.8	0.5	1.5	1.266667	0.9	0.5	0.3	0.566667	NPA
8	A8	216.8	6.1631	7.0623	7.2	7.2	7.2	7.2	2	1.5	1.8	1.766667	0.2	0.5	0.4	0.366667	NPA
9	B1	199	6.2261	7.0434	4.1	5.2	5	4.766667	1.1	0.8	1	0.966667	1.2	1	0.8	1	SH
10	B2	200.3	6.2367	7.0554	6.4	6.6	5.8	6.266667	1.4	1	1.3	1.233333	1	0.8	0.9	0.9	PA
11	B3	199.4	6.2362	7.0296	5.9	5.4	5.7	5.666667	0.5	0.8	0.9	0.733333	0.6	0.4	0.3	0.433333	PA
12	B4	204.3	6.2192	7.0535	6.1	6.6	5.9	6.2	0.9	0.5	1.1	0.833333	0.8	0.4	0.5	0.566667	PA
13	B5	206.2	6.2137	7.0317	6.3	5.8	6.3	6.133333	1.3	1	0.7	1	0.9	0.5	0.3	0.566667	PA
14	B6	229.1	6.1562	7.0227	6.8	6.8	6.7	6.766667	1.1	1	1.7	1.266667	0.4	0.3	0.6	0.433333	NPA
15	B7	227.1	6.1429	7.0319	4.8	5.5	4.5	4.933333	0.4	1.4	1.6	1.133333	0.8	0.6	0.4	0.6	NPA
16	B8	231.6	6.1351	7.0186	5.2	5.1	5.2	5.166667	0.7	1.3	1	1	0.7	0.4	0.2	0.433333	NPA
17	C1	237.1	6.0941	7.0241	4.8	5.4	5.1	5.1	1.9	1.6	1.2	1.566667	0.9	0.5	0.6	0.666667	SH
18	C2	238.2	6.0923	7.0223	4.9	4.9	4.6	4.8	1.8	1.5	1.2	1.5	0.7	0.3	0.4	0.466667	PA
19	C3	230.1	6.0983	7.0204	5.5	5.3	4.2	5	1.5	1.8	1.5	1.6	0.5	0.4	0.2	0.366667	PA

S/N	Code	Elevation	Latitude	Longitude	pH			Mean	Al			Mean	H			Mean	Remark
					Soil Depth (ft)				Soil Depth (ft)				Soil Depth (ft)				
					0.5	1.5	2.5		0.5	1.5	2.5		0.5	1.5	2.5		
20	C4	242.1	6.0854	7.0315	7.1	6.9	6.9	6.966667	1.5	1	1.4	1.3	0.3	0.2	0.5	0.333333	PA
21	C5	244.4	6.0757	7.0191	6.5	6.3	6	6.266667	1.9	1.5	1.3	1.566667	0.2	0.2	0.7	0.366667	PA
22	C6	240	6.1346	7.0001	4.9	4.7	4.4	4.666667	1.5	1.3	1	1.266667	0.7	0.5	0.6	0.6	NPA
23	C7	241.4	6.1024	6.9827	4.9	5.2	5.1	5.066667	1.2	1.5	0.8	1.166667	0.8	0.6	0.5	0.633333	NPA
24	C8	241	6.0753	6.9933	5.1	5.1	5.2	5.133333	1.3	1.8	1.5	1.533333	0.5	0.3	0.5	0.433333	NPA

Table 4: Mean Values of Potassium, Sodium and Calcium at different depth in cmol/kg

S/N	Code	Elevation	Latitude	Longitude	K			Mean	Na			Mean	Ca			Mean	Remark
					Soil Depth (ft)				Soil Depth (ft)				Soil Depth (ft)				
					0.5	1.5	2.5		0.5	1.5	2.5		0.5	1.5	2.5		
1	A1	212.9	6.1967	7.0959	0.31	0.32	0.11	0.246667	0.25	0.15	0.11	0.17	0.8	0.5	1	0.766667	SH
2	A2	216.3	6.1916	7.0936	0.33	0.1	0.03	0.153333	0.35	0.4	0.12	0.29	0.7	0.2	1.5	0.8	PA
3	A3	218.2	6.1884	7.1028	0.71	0.51	0.62	0.613333	2.5	1.65	1.5	1.883333	2.7	2.5	2	2.4	PA
4	A4	209.8	6.2063	7.0936	0.51	0.5	0.48	0.496667	2.4	2	1.8	2.066667	2.5	2.3	2	2.266667	PA
5	A5	210.1	6.2045	7.1055	0.17	0.18	0.09	0.146667	0.21	0.31	0.24	0.253333	1.3	1	1.5	1.266667	PA
6	A6	229.9	6.1134	7.0577	0.41	0.21	0.54	0.386667	0.48	0.45	0.52	0.483333	1.9	1.5	1.2	1.533333	NPA
7	A7	225.8	6.1217	7.0715	0.32	0.32	0.13	0.256667	1.54	1.41	0.55	1.67	2	1.7	1.2	1.633333	NPA
8	A8	216.8	6.1631	7.0623	0.72	0.72	0.62	0.686667	2.8	1.7	1.8	2.1	2.8	2.5	2.2	2.5	NPA
9	B1	199	6.2261	7.0434	0.21	0.15	0.08	0.146667	0.1	0.15	0.2	0.15	0.9	1.2	1.5	1.2	SH
10	B2	200.3	6.2367	7.0554	0.51	0.42	0	0.31	0.32	0.2	0.3	0.273333	1.3	0.4	1.5	1.066667	PA
11	B3	199.4	6.2362	7.0296	0.35	0.3	0.23	0.293333	0.25	0.2	0.52	0.323333	1.3	1	0.7	1	PA
12	B4	204.3	6.2192	7.0535	0.42	0.31	0.15	0.293333	0.21	0.21	0.41	0.276667	1.7	1.5	1.2	1.466667	PA
13	B5	206.3	6.2137	7.0317	0.13	0.54	0.58	0.416667	0.41	0.32	0.25	0.326667	0.8	0.6	1.8	1.066667	PA
14	B6	229.1	6.1562	7.0227	0.62	0.55	0.65	0.606667	2.6	1.7	1.94	2.08	2.5	1.7	2	2.066667	NPA
15	B7	227.1	6.1429	7.0319	0.41	0.12	0.08	0.203333	1.2	1.21	1.3	1.236667	2	1.2	0.8	1.333333	NPA
16	B8	231.6	6.1351	7.0186	0.41	0.53	0.59	0.51	1.82	1.51	0.44	1.256667	1.9	1.5	2	1.8	NPA
17	C1	231.1	6.0941	7.0241	0.15	0.33	0.21	0.23	0.91	0.76	0.5	0.723333	0.5	0.2	0.09	0.263333	SH
18	C2	238.2	6.0923	7.0223	0.21	0.2	0.05	0.153333	1.21	0.43	0.76	0.8	0.9	0.3	1.8	1	PA
19	C3	230.1	6.0983	7.0204	0.62	0.15	0.2	0.323333	1.45	0.81	0.56	0.94	0.7	1.2	0.5	0.8	PA
20	C4	242.1	6.0854	7.0315	0.73	0.61	0.51	0.616667	2.45	2.01	2.31	2.256667	1.8	1.3	0.7	1.266667	PA
21	C5	244.4	6.0757	7.0191	0.63	0.54	0.61	0.593333	2.36	2.21	2.51	2.36	1.5	0.6	1.3	1.133333	PA
22	C6	240.1	6.1346	7.0001	0.12	0.13	0.15	0.133333	2.9	2	1.81	2.236667	2	0.4	1.7	1.366667	NPA
23	C7	241.4	6.1024	6.9827	0.52	0.2	0.11	0.276667	1.47	1.52	2	1.663333	1.6	1.2	0.7	1.166667	NPA
24	C8	241.5	6.0753	6.9933	0.32	0.3	0.01	0.21	1.12	1.02	1.65	1.263333	2	1.8	1.8	1.866667	NPA

Table 4: Mean Values of Magnesium, Effective Cation Exchange capacity and Base Saturation at different Soil Depth

S/N	Code	Elevation	Latitude	Longitude	Mg			Mean	ECEC			Mean	BS			Mean	Remark
					Soil Depth(ft)				Soil Depth (ft)				Soil Depth (ft)				
					0.5	1.5	2.5		0.5	1.5	2.5		0.5	1.5	2.5		
1	A1	212.9	6.1967	7.0959	0.5	0.3	0.5	0.433333	1.86	1.27	1.72	1.616667	30.2	25.2	32.1	29.16667	SH
2	A2	216.3	6.1916	7.0936	0.4	0.2	0.4	0.333333	1.78	0.9	2.05	1.576667	30.3	20.3	14.3	21.63333	PA
3	A3	218.2	6.1884	7.1028	2.5	1.9	2	2.133333	6.82	5.56	5.34	5.906667	45.2	42.1	36.7	41.33333	PA
4	A4	209.8	6.2063	7.0936	2.3	2.4	2.2	2.3	6.12	5.72	5.22	5.686667	50.3	45.8	40.2	45.43333	PA
5	A5	210.1	6.2045	7.1055	1.8	1.5	1.3	1.533333	3.48	2.99	3.13	3.2	30.1	20.1	27.2	25.8	PA
6	A6	229.9	6.1134	7.0577	1.6	1.4	1.5	1.5	4.39	3.56	3.76	3.903333	25.3	15.9	10.3	17.16667	NPA
7	A7	225.8	6.1217	7.0715	1.3	1.6	1.4	1.433333	4.16	4.03	3.28	3.823333	38.3	20.2	15.2	24.56667	NPA
8	A8	216.8	6.1631	7.0623	2.5	2.5	1.9	2.3	6.83	6.44	5.53	6.266667	51.2	39.5	30.4	40.36667	NPA
9	B1	199	6.2261	7.0434	0.6	0.5	0.7	0.6	1.81	2	2.48	2.096667	25.2	15.3	20.2	20.23333	SH
10	B2	200.3	6.2367	7.0554	0.3	0.8	0.6	0.566667	2.43	1.82	2.4	2.216667	29.3	20.1	15.3	21.56667	PA
11	B3	199.4	6.2362	7.0296	1.2	1.3	1.5	1.333333	3.1	2.8	25.72	10.54	33.2	25.3	20.2	26.23333	PA
12	B4	204.3	6.2192	7.0535	0.5	0.6	1.2	0.766667	2.83	2.62	2.96	2.803333	24.3	19.3	22.5	22.03333	PA
13	B5	206.2	6.2137	7.0317	1.3	0.9	1.5	1.233333	2.64	2.36	4.13	3.043333	25.7	20.5	30.1	25.43333	PA
14	B6	229.1	6.1562	7.0227	2.4	2.1	2.5	2.333333	6.15	5.06	5.8	5.67	42.6	34.2	42.6	39.8	NPA
15	B7	227.1	6.1429	7.0319	0.9	0.5	1.3	0.9	3.51	2.03	2.48	2.673333	35.2	23.9	18.4	25.83333	NPA
16	B8	231.6	6.1351	7.0186	2.1	0.9	1.5	1.5	4.83	3.44	4.53	4.266667	36.2	21.4	15.2	24.26667	NPA
17	C1	237.1	6.0941	7.0241	0.4	0.5	1.2	0.7	1.96	2.24	3.15	2.45	45.6	31.2	25.3	34.03333	SH
18	C2	238.2	6.0923	7.0223	0.8	0.3	0.8	0.633333	3.12	2.32	4.39	3.276667	43.2	20.5	10.4	24.7	PA
19	C3	230.1	6.0983	7.0204	0.9	0.5	1.6	1	3.67	2.66	2.86	3.063333	40.4	39.2	20.1	33.23333	PA
20	C4	242.1	6.0854	7.0315	2	1.5	2.3	1.933333	6.98	5.42	5.82	6.073333	61.2	48.5	60.2	56.63333	PA
21	C5	244.4	6.0757	7.0191	1.9	1.4	1.5	1.6	6.39	4.75	5.92	5.686667	57.8	44.2	37.8	46.6	PA
22	C6	240	6.1346	7.0001	0.4	0.6	0.6	0.533333	4.04	2.75	4.26	3.683333	39.2	24.5	17.4	27.03333	NPA
23	C7	241.4	6.1024	6.9827	0.9	0.5	1.2	0.866667	4.49	3.42	4.01	3.973333	40.1	29.4	19.3	29.6	NPA
24	C8	241	6.0753	6.9933	0.3	0.7	0.4	0.466667	3.74	3.82	3.86	3.806667	37.2	30.2	35.2	34.2	NPA

DISCUSSION

The soils within the study area exhibit a prominent sandy composition, which follows a decreasing trend as depth increases, as illustrated in Table 3. This noteworthy characteristic can be attributed to the study area's proximity to the origin of Nanka sands. These sands have their source in the Imo shale, a shale unit that stems from a coastal sandy mudstone. It is worth emphasizing the unique porous structure of the Nanka sands, characterized by coarse-grained and pebbly quartz sands. The relatively low presence of silt and clay soils in the study area can be ascribed to the susceptibility of the soil to leaching, a process that is common in the Nanka sandy zones. Leaching contributes to the soil's (clay soil) unstable nature in these areas, consequently accentuating the predominance of sandy composition. The leaching process entails the removal of mineral and organic substances from the soil profile, leading to reduced nutrient retention and increased vulnerability to erosion and nutrient depletion [47]. The relatively low presence of organic carbon/matter in the study area can be attributed to a combination of natural processes and human activities, each playing a significant role in its decline. These factors encompass sheet erosion, leaching of the soil (as explained) and urbanization. Sheet erosion, a process whereby thin layers of soil are removed by flowing water, plays a significant role in the dispersal of soil particles and nutrient, thus, it reduces both the organic carbon and matter, as top soil and vegetative cover are lost in the process. The resulting dispersal of soil particles carries away valuable organic matter, diminishing its overall quantity. Similarly, leaching, the movement of water through the soil, further contributes to the reduction of organic matter by washing away dissolved organic substances. Human activities, particularly the rapid expansion of urban structures, also contribute to the decline in organic matter levels in the study areas. The expansion of urban areas results in the removal of natural vegetation cover, which plays a crucial role in the accumulation and preservation of organic carbon. The loss of vegetative cover exacerbates the decline in organic matter, as it reduces the input of organic materials into the soil through the decomposition of plant residues.

According to the research conducted by [54], soils with organic matter levels below 2% are considered to be at their critical level. Furthermore, [55] suggests that soils with organic carbon content below 3.5% can be classified as having erodible properties. When examining the distribution of organic carbon (OC) and organic matter (OM) based on the values presented in Table 2, it becomes evident that there is no discernible pattern or order. Both low and extreme low values of OC and OM are observed in areas affected by soil piping as well as non-piping areas across different regions, these result obtained is similar to the works [1, 21]. The analysis of figures in the study area reveals a consistently low amount of total nitrogen, indicating significant leaching in the soil (Table 2). Approximately 95% of the

nitrogen found in the soil is deposited within the organic matter [22]. However, the rise of deforestation in the state has led to a reduction in vegetative cover, resulting in a decrease in organic matter content. Consequently, this diminishes the soil's ability to resist leaching. Urbanization, a key driver of erosion in the state, is closely correlated with soil leaching and can be evaluated through the assessment of nitrogen levels in the soil. Erosion plays a significant role in leaching, particularly concerning the water-soluble forms of nitrogen such as nitrate and ammonium. Excess water moving through the soil decomposes soil nutrients, leading to the leaching of these nitrogen compounds. Interestingly, the highest values of total nitrogen are observed within the non-piping regions of the study areas. These regions can be considered as parts of the study area where there is minimal detachment of soils for particle transportation. Conversely, areas with very low nitrogen levels are indicative of prevalent erosion and leaching processes. Piping, a phenomenon characterized by the formation of underground channels, typically occurs in these areas. The pH level of soil serves as an indicator of its acidity or alkalinity table 3. Soils that contain high level of salt tend to have an elevated pH value.

The accumulation of sodium in the soil occurs when water faces difficulty infiltrating through the soil matrix. This phenomenon is associated with various physical processes, including soil dispersion, clay platelet swelling, and aggregate swelling. These processes are particularly prominent in areas with high exchange cations content, such as the Agulu site (Table 4). The detrimental effects of excessive sodium accumulation in the soil can be attributed to the disruption of the forces that bind clay particles together. When an excessive number of sodium ions come between the clay particles, these forces are weakened, resulting in the expansion, swelling, and dispersion of the particles [9]. Consequently, the soil pores become blocked, impeding the movement of water into and through the soil. The consequences of this sodium-induced soil structure alteration are significant. The obstruction of soil pores leads to the phenomenon of runoff, where water is unable to infiltrate the soil and instead flows over the surface. This runoff not only contributes to the loss of topsoil but also hampers the natural movement of water through the soil profile. The study areas under investigation exhibit high levels of sodium and base saturation, with the Agulu site displaying particularly elevated concentrations. The effective cation exchange capacity (ECEC) of a soil refers to its overall capacity to retain exchangeable cations. These exchangeable cations encompass a range of essential elements, including calcium, magnesium, potassium, sodium, hydrogen, and aluminum (to name a few that were specifically analyzed in this research). The binding of these cations is facilitated by the presence of negatively charged particles within the soil matrix. Soils that possess higher proportions of clay fractions, and organic matter values tend to exhibit elevated levels of

ECEC. This is due to the increased availability of negatively charged particles within these soil types, which can effectively retain a greater quantity of exchangeable cations. The implications of having a high ECEC within a soil are noteworthy. Soils with higher ECEC values tend to display enhanced compaction and possess a greater capacity to retain water. Conversely, soils with lower ECEC values are more prone to leaching and can lose essential nutrients more readily. In the study areas under investigation, the general levels of exchangeable cations and ECEC are relatively low, with the exceptions of B6 and the Agulu zones where the values tend to be average (as indicated in Table 5).

CONCLUSION

This research presents a comprehensive and meticulous investigation into the chemical characteristics of soils in the vicinity of sinkholes situated in Anambra State, Nigeria. From the findings derived from this study it was established that areas distant from the sinkhole sites exhibited low values of exchangeable bases, high levels of sodium content, and pH imbalances. Consequently, these factors led to soil dispersion and swelling, resulting in inadequate water infiltration and heightened run-off. The cumulative effect of these processes culminated in tunnel erosion, eventually leading to the formation of sinkholes. The implications of these findings are significant, as they provide valuable insights into the mechanisms driving sinkhole formation and expansion. By identifying the correlation between low exchangeable bases, elevated sodium levels, and pH imbalances with soil dispersion and reduced infiltration, this research paves the way for implementing targeted interventions to mitigate the occurrence of sinkholes. Such interventions may include improved soil management practices, enhanced water infiltration measures, and the establishment of appropriate land-use policies. It is crucial to acknowledge that the study's outcomes have implications that extend beyond the specific study area in Anambra State, Nigeria. The insights gained from this research can inform similar investigations in other regions prone to sinkhole formation, thereby contributing to a broader understanding of this geological phenomenon.

Conflicts of Interest

There are no conflicts of interest among the authors.

REFERENCES

1. Ayadiuno, R.U. (2021). "Analysis of Soil Erosion Causative Factors and Susceptibility in Anambra State, Southeastern, Nigeria. *Biosc Biotech Res Comm*, 14(9), pp. 212–218.
2. Ayadiuno, R. U., Ndulue, D. C., Ndichie, C. C., Mozie, A. T., Phil-Eze, P. O., & Onyekwelu, A. C. (2021). Geospatial Analysis of Soil Erosion Susceptibility and Causative Factors in Anambra State, South East, Nigeria. *Scientific Review*. 2021b, 8(1), 5-32.
3. Bernatek-Jakiel, A., & Poesen, J. (2018). Subsurface erosion by soil piping: significance and research needs. *Earth-Science Reviews*, 185, 1107-1128.
4. Chibuogwu, I. U., and Ugwu, G. Z. (2023). "Uncovering soil piping vulnerability using direct current geophysical techniques in Awka, Anambra State, Nigeria. *IJMARGE*, 4(3), pp. 426–450.
5. Hardie, M. A., Cotching, W. E., & Zund, P. R. (2007). Rehabilitation of field tunnel erosion using techniques developed for construction with dispersive soils. *Soil Research*, 45(4), 280-287.
6. Research on Soil Piping – Kerala State Disaster Management Authority. <https://sdma.kerala.gov.in/research-on-soil-piping/> (accessed Aug. 28, 2023).
7. Bryan, R. B. (1997). The significance of soil piping processes: inventory and prospect. *Geomorphology*, 20, 209-218.
8. García-Ruiz, J., Lasanta, T., & Alberto, F. (1997). Soil erosion by piping in irrigated fields. *Geomorphology*, 20(3-4), 269-278.
9. Hardie, M. (2009). *Dispersive soils and their management*. Technical Reference Manual.
10. Fitzpatrick, R. W., Boucher, S. C., Naidu, R., & Fritsch, E. (1994). Environmental consequences of soil sodicity. *Soil Research*, 32(5), 1069-1093.
11. Rengasamy, P., Greene, R., Ford, G., and Mehanni, A. (1984). "Identification of dispersive behaviour and the management of red-brown earths. *Soil Res.*, 22(4), p. 413.
12. Green, R. (1962). "Infiltration of water into soils as influenced by antecedent moisture. Accessed: Aug. 25, 2023. [Online]. Available: <https://dr.lib.iastate.edu/handle/20.500.12876/73601>
13. Cleophas, F., Isidore, F., Musta, B., Ali, B. M., Mahali, M., Zahari, N. Z., & Bidin, K. (2022, August). Effect of soil physical properties on soil infiltration rates. In *Journal of Physics: Conference Series* (Vol. 2314, No. 1, p. 012020). IOP Publishing.
14. Ma, W., Zhang, X., Zhen, Q., & Zhang, Y. (2016). Effect of soil texture on water infiltration in semiarid reclaimed land. *Water Quality Research Journal of Canada*, 51(1), 33-41.
15. Ocheli, A., Ogbe, O. B., & Aigbadon, G. O. (2021). Geology and geotechnical investigations of part of the Anambra Basin, Southeastern Nigeria: implication for gully erosion hazards. *Environmental Systems Research*, 10(1), 1-16.
16. Ola-Buraimo, A. O., & Akaegbobi, I. M. (2013). Palynological evidence of the oldest (Albian) sediment in the Anambra Basin, southeastern Nigeria. *Journal of Biological and Chemical research*, 30(2), 387-408.
17. Adeigbe, O. C., & Salufu, A. E. (2009). Geology and Depositional Environment of Campano-Maastrichtian sediments in the Anambra Basin,

- southeastern Nigeria: Evidence from field relationship and sedimentological study. *Earth Sciences Research Journal*, 13(2), 148-165.
18. Madukwe, H. Y. (2020). Provenance and tectonic setting of the Eocene Nanka Sandstone, Anambra Basin, Nigeria. *Transactions of the Royal Society of South Africa*, 75(1), 54-63.
 19. USEPA, "USEPA Document." U.S Environmental Protection Agency, 2021.
 20. Ejikeme, C., Nweke, I. (2016). "Physical and Chemical Characterisation of Soils of Anambra State College of Agriculture, Mgbakwu. *GJAS*, 6(10), pp. 326–330.
 21. Ayadiuno, R. U., & Ndulue, D. C. (2021). An Investigation into some Soil Indices as Indicators of High Soil Erodibility in Anambra State Southeastern, Nigeria. *International Journal of Modern Agriculture*, 10(2), 3451-3464.
 22. Norén, I. S., van Geel, W., and de Haan, J. (2021). "Cover crop reference values: Effective organic matter and nitrogen uptake. doi: 10.18174/544859.